

# 단상 계통연계 인버터를 위한 개선된 고조파 보상법

칸 레이안<sup>1</sup>, 최우진<sup>†</sup>

## An Improved Harmonic Compensation Method for a Single-Phase Grid Connected Inverter

Reyyan Ahmad Khan<sup>1</sup> and Woojin Choi<sup>†</sup>

### Abstract

Grid-connected inverters should satisfy a certain level of total harmonic distortion (THD) to meet harmonics standards, such as IEEE 519 and P1547. The output quality of an inverter is typically degraded due to grid voltage harmonics, dead time effects, and the device's turn-on/turn-off delay, which all contribute to increasing the THD value of the output. The use of a harmonic controller is essential to meet the required THD value for inverter output under a distorted grid condition. In this study, an improved feedforward harmonic compensation method is proposed to effectively eliminate low-order harmonics in the inverter current to the grid. In the proposed method, harmonic components are directly compensated through feedforward terms generated by the proportional resonant controller with the grid current in a stationary frame. The proposed method is simple to implement but powerful in eliminating harmonics from the output. The effectiveness of the proposed method is verified through simulation using PSIM software and experiments with a 5 kW single-phase grid-connected inverter.

**Key words:** SPGCI(Single Phase Grid Connected Inverter), Harmonic compensation method, THD(Total Harmonic Distortion), Harmonic standard

### 1. Introduction

Majority portion of the conventional energy resources such as natural gas, petroleum, and coal are used to generate the power for residences and industries, and it generates a significant amount of carbohydrates and other toxic gases as by-products. As a result, these affect significantly on the environment which leads to the global warming. In this circumstance it has become essential to find out the alternate way to generate and utilize the energy such as

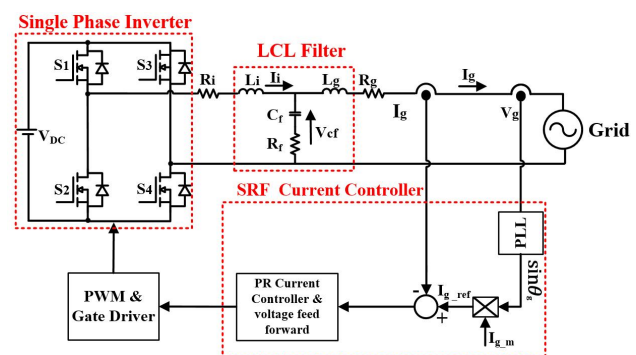


Fig. 1. Stationary reference frame(SRF) current controller for single phase GCIs.

the renewable energy and Distributed Generation(DG).

Recently, the use of DG systems based on wind energy, solar energy and other renewable energy resources has been greatly increased<sup>[1]-[4]</sup>. In the DG systems, the Grid Connected Inverter(GCI) is a key element<sup>[5]</sup>, it plays a role to extract the maximum available power from the energy sources and to transfer

Paper number: TKPE-2019-24-3-10

Print ISSN: 1229-2214 Online ISSN: 2288-6281

<sup>†</sup> Corresponding author: cwj777@ssu.ac.kr, Dept. of Electrical Engineering, Soongsil University

Tel: +82-2-820-0652 Fax: +82-2-817-7961

<sup>1</sup> Dept. of Electrical Engineering, Soongsil University

Manuscript received Nov. 8, 2018; revised Nov. 16, 2018; accepted Dec. 26, 2018

— 본 논문은 2018년 전력전자학술대회 우수추천논문임

— 본 논문은 2018년 전력전자학술대회 태양광논문상 수상논문임

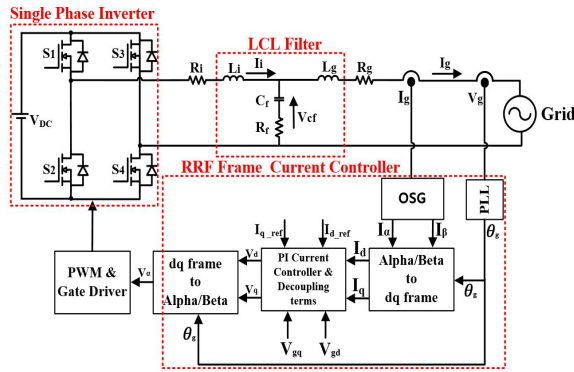


Fig. 2. Rotating reference frame(RRF) current controller for single phase GCIs.

it to the utility grid. However, increasing use of inverter based DG systems causes a power quality issue in the grid due to the harmonics present in its output. There are other factors which also degrade the output quality of GCI such as the dead band of PWM, the turn-on/turn-off delays of the switches, the dc-offset and the scaling error in the current and voltage sensing circuits, and so on<sup>[6]</sup>. Typically, the performance of the current injected into the utility grid is assessed by the Total Harmonic Distortion (THD). According to IEEE-1547 and IEEE-519, the THD value of the grid current should be less than 5%<sup>[7],[8]</sup>. In order to meet the THD of the injected current to the grid suggested by the codes, a suitable current control strategy should be employed<sup>[9]-[13]</sup>. In recent years, various current control methods for single phase GCI have been presented in the literature. The current control methods can be categorized into two main kinds based on the reference frame to be used for the control.

The stationary reference frame(SRF) current controller is simple to implement and has less computational burden as shown in Fig. 1. In the SRF current control scheme the proportional-integral(PI) current controller is often used since it is simple to implement and has a good performance. One of the main drawbacks of the method is that the performance of the SRF based control heavily depends on the system bandwidth. Therefore, the bandwidth of the PI controller should be high enough to follow the AC reference with a negligible error. However, it may not be possible to select the high enough bandwidth for the high power applications due to the limitation of the switching frequency. Therefore, it is not preferred to control the inverter in the SRF<sup>[14]-[16]</sup>. Due to the problem mentioned above the Proportional

Resonant(PR) controller is preferred to control the inverter in the SRF<sup>[17]-[19]</sup>. Unlike the conventional PI current controller it can track the sinusoidal reference of arbitrary frequency with zero steady-state error by introducing an infinite gain at the desired resonant frequency. Due to its very high gain at the desired resonant frequency it can be used to compensate the low order harmonics by connecting it in parallel with the current controller<sup>[20]</sup>.

However, the difficulty in implementing the PR controller is to discretize the controller because it has a narrow band and infinite gain at the resonant frequency. Actually, a slight disagreement of the resonant pole may cause a significant loss in terms of performance. Even under the small frequency deviation in the resonant frequency, the controller behaves like a proportional controller and it is not able to achieve zero steady-state error. The sensitivity of PR controller can be reduced to increase the robustness towards frequency variation by adding a damping factor. However, the damping factor should be selected carefully because inappropriate selection of the damping factor results in an amplification of the undesired frequencies and noise, which provides the detrimental effects to the control performance<sup>[20],[21]</sup>.

In order to overcome the problems associated with the SRF based current controller, the Rotating Reference Frame(RRF) based current controller has been introduced as shown in Fig. 2<sup>[22]-[24]</sup>. Initially, the RRF current controller has been introduced for the control of three phase systems. In the RRF controllers, since the  $\alpha\beta/dq$  transformation turns ac quantities into dc quantities, a good control performance can be achieved with PI controllers. The design process of the PI controller is simple and it provides satisfactory dynamic and steady-state performance. Also, as the system variables are converted to dc quantities, the control loop has no dependence on the system frequency. In addition, in this scheme independent regulation for active and reactive power can be achieved by the simple adjustment of the d and q axis current. Although the computational burden of the RRF based current controller is higher than that of the SRF based PR controller due to the axis transformation, its implementation has become easier thanks to the availability of the high performance DSP with low cost.

The RRF based current control method can be

applied to the single phase GCIs. To control the single phase inverter in the RRF the Orthogonal Signal Generator(OSG) is required. Conventionally, OSG is implemented using phase shift methods such as the Hilbert transform<sup>[25]-[27]</sup>, the time delay<sup>[28]</sup> or the all-pass filter<sup>[29]</sup>. These techniques work fine under the pure sinusoidal inverter output current. However, when the harmonics are present in the grid inject current, these techniques are not able to generate the perfect orthogonal signal, thereby causing a steady state error. The other method to extract the orthogonal signals from the inverter output current named by Second-Order Generalized Integrator(SOGI) is proposed<sup>[30]</sup> and it is widely used since it generates the OSG signals perfect. Furthermore, it provides good harmonic attenuation.

The inverter current injected into the grid gets polluted due to the harmonics present in the grid voltage along with the others detrimental factors. Under these conditions the conventional RRF current controllers are not able to work perfectly. In order to improve the output quality of the GCIs under the distorted grid conditions, an advanced current control method need to be employed. One approach introduced in<sup>[31]</sup> employs a PR controller connected in parallel with a PI controller in d and q axis, respectively. In this approach the PI controller act as a current regulator while the PR controller extracts the specific ac ripple from each d and q axis and compensate it in the closed loop with negative feedback. In addition, since a harmonic component in the SRF appears as two different components in the RRF, two harmonic compensators are required to eliminate a certain harmonic for each d and q axis. This makes it quite complex to design and to implement the harmonic compensators. In the SOGI based harmonic compensation method introduced in<sup>[32]</sup>, a SOGI block connected in parallel with a current regulator for each d and q axis to eliminate a certain harmonic. This method provides desirable performance in terms of harmonic rejection. However, a low pass filter and a bandpass filter included in the SOGI block make the control method complicated and increase the computational burden. The other approach uses a method to detect the individual harmonic at its own frequency frame and to compensate it after converting it to a dc component.<sup>[33]</sup> However, it is disadvantageous in that its computational burden is high due to the use of multiple numbers of RRFs and its dynamic

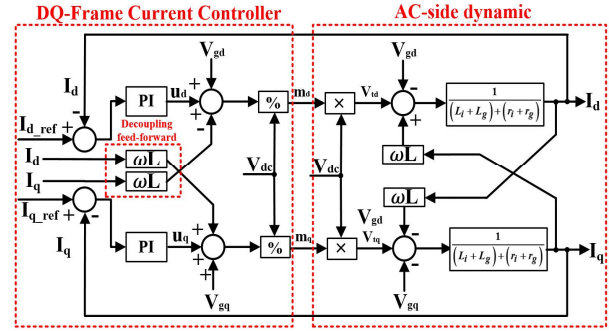


Fig. 3. Control block diagram of a current controller in RRF.

performance is not good due to the delay produced by the low pass filter.

In this paper, an advanced harmonic compensation method is introduced to overcome the drawbacks of the conventional methods. In the proposed method, the multi-resonant harmonic controller is implemented to effectively mitigate the low order harmonics in SRF with PI current controller in RRF. Furthermore, the proposed control technique is quite simple and has low computational burden as compared to the conventional approaches.

The paper is organized as follows: An overview of the conventional current controller for a single phase inverter in RRF is shown in section 2. In section 3 harmonic compensation methods for a single phase inverter are discussed. In section 4 and 5 simulation and experimental results are presented to validate the effectiveness of the proposed method. Finally, the conclusion is made in section 6.

## 2. Conventional Current Controller Based on RRF for Single Phase Grid Connected Inverters

A general block diagram of the current controller in RRF is shown in Fig. 2, where the inverter is interfaced to the grid through an LCL passive filter. Based on Fig. 2 the dynamic equations for the ac side can be described as:

$$V_{inv} = R_i I_i + s L_i I_i + V_{cf} \quad (1)$$

$$V_{cf} = R_g I_g + s L_g I_g + V_g$$

$$I_i = I_g + C_f \frac{V_{cf}}{s}$$

Where,  $V_{inv}$ ,  $V_{cf}$ ,  $V_g$ ,  $I_i$  and  $I_g$  represent the inverter terminal voltage, the capacitor voltage, the utility grid

voltage, the converter-side current and the grid current, respectively. If the influence of the capacitor in the current control design is neglected, the design of current control is the same as for voltage source inverter with an L filter. Thus, in the  $\alpha$ - $\beta$  frame, Eq. (1) can be simplified to Eq. (2).

$$V_{inv.\alpha} = (R_i + R_g)I_\alpha + s(L_i + L_g)I_\alpha + V_{g.\alpha} \quad (2)$$

$$V_{inv.\beta} = (R_i + R_g)I_\beta + s(L_i + L_g)I_\beta + V_{g.\beta}$$

Further, after applying a stationary-to-rotating transformation to Eq. (2), the dynamic of the ac-side variable in the rotating-frame(dq frame) can be derived as Eq. (3).

$$V_{inv.d} = (R_i + R_g)I_d + s(L_i + L_g)I_d - \omega_{ff}(L_i + L_g)I_q + V_{g.d} \quad (3)$$

$$V_{inv.q} = (R_i + R_g)I_q + s(L_i + L_g)I_q + \omega_{ff}(L_i + L_g)I_d + V_{g.q}$$

The system in the RRF based on Eq. (3) including the typical compensation and the decoupling terms can be illustrated as shown in Fig. 3. In order to achieve a decoupling control of  $I_d$  and  $I_q$  the inverter terminal voltage should be controlled as follows:

$$V_{inv.d} = u_d - \omega_{ff}(L_i + L_g)I_q + V_{g.d} \quad (4)$$

$$V_{inv.q} = u_q + \omega_{ff}(L_i + L_g)I_d + V_{g.q}$$

where  $u_d$  and  $u_q$  is the control signal of the d and q axis in the RRF, respectively. From Eq. (3) and Eq. (4), the decoupling system in Eq. (5) can be deduced.

$$u_d = (R_i + R_g)I_d + s(L_i + L_g)I_d \quad (5)$$

$$u_q = (R_i + R_g)I_q + s(L_i + L_g)I_q$$

Eq. (5) describes two decoupled, first-order, linear systems. Based on Eq. (5),  $i_d$  and  $i_q$  can be controlled by  $u_d$  and  $u_q$ , respectively. Fig. 3 shows a block representation of the d and q axis current controller of the GCI system where  $u_d$  and  $u_q$  are the output of two corresponding PI current controllers. To cancel the effect of grid voltage and decoupling terms present in the plant, these terms are added in the current controller to perfectly cancel each other. Therefore Fig. 3 can be simplified as Fig. 4.

Fig. 4 indicates that the both d and q axis current-control loops are identical. Therefore, the

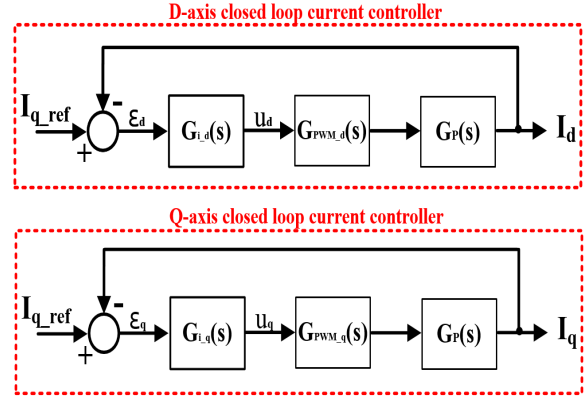


Fig. 4. Simplified block diagram of a current controller.

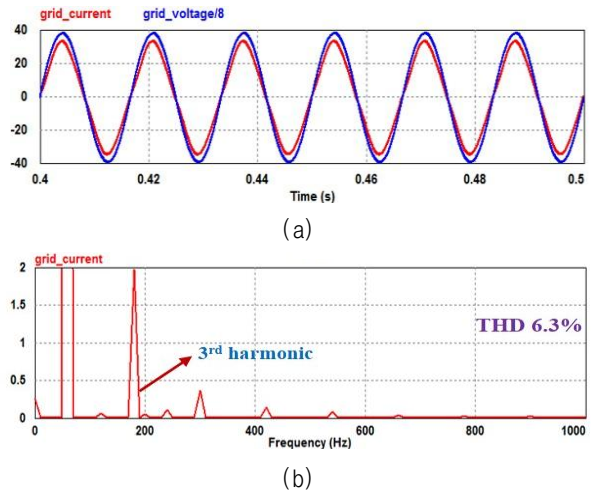


Fig. 5. Simulation result of a current controller without a harmonic controller at 5kW.

corresponding compensators are also identical. Here,  $G_{PWM}(s)$  is the transfer functions of the PWM unit in the  $s$ -domain, which includes the computation delay, sampler and zero-order hold unit as shown in Eq. (6).

$$G_{PWM}(s) = \frac{e^{-T_s s}(1 - e^{-T_s s})}{T_s s} \approx \frac{(1 - 0.5T_s s)}{(1 + 0.5T_s s)^2} \quad (6)$$

Where,  $T_s$  is the sample time. The loop gain for the whole system can be expressed by Eq. (7).

$$G_o(s) = G_i(s) * G_{PWM}(s) * G_p(s) \quad (7)$$

The output regulation performance can be improved by adding the cross-coupling terms in a feedforward manner. While the performance of the current controller is good enough only with fundamental frequency components, it becomes poor when the harmonics are present in the grid due to the limited bandwidth of the PI controller.

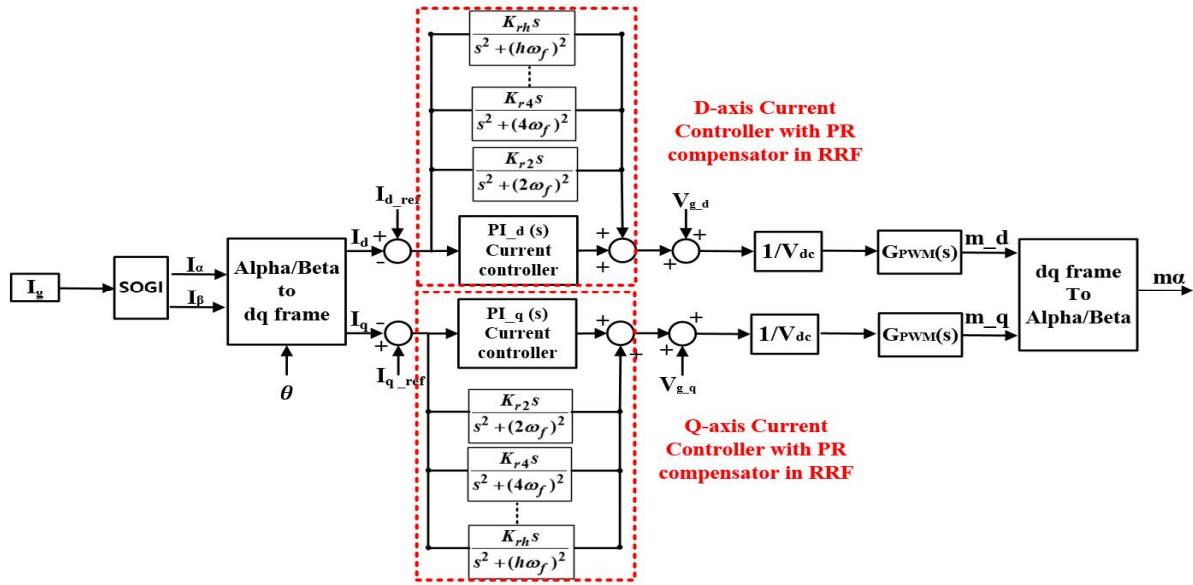


Fig. 6. Block diagram of the conventional harmonic compensation method in RRF.

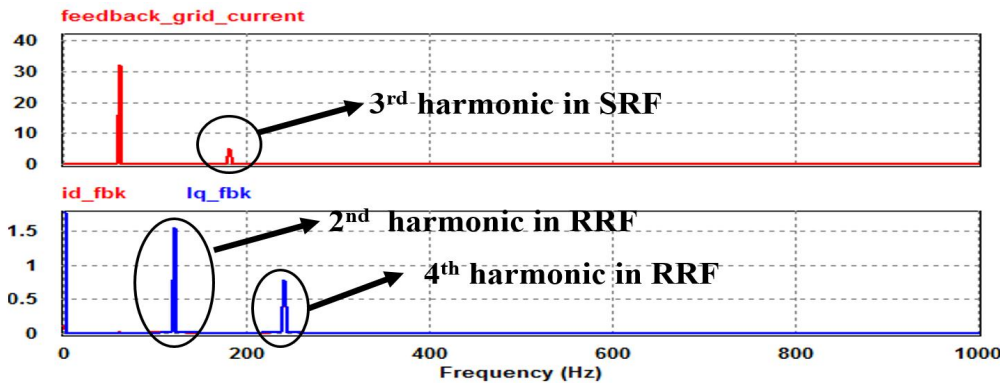


Fig. 7. FFT analysis of 3<sup>rd</sup> harmonic in SRF and RRF.

Fig. 5 shows the simulation results of conventional RRF current controller under the presence of the harmonics such as 2<sup>nd</sup>, 3<sup>rd</sup> and 5<sup>th</sup> harmonics with 0.1%, 0.4% and 0.1% of the grid voltage, respectively. The THD is about 0.5% and the dead time is 0.5 $\mu$ s. In this case THD of the inverter output current is 6.3% and the amplitude of the 3<sup>rd</sup> harmonic is 1.96A, which doesn't satisfy the IEEE 519 and P1547 harmonic standards. Therefore, additional controllers for the harmonic compensation is needed to meet the harmonic standard under non-sinusoidal grid condition.

### 3. Harmonic Compensation Methods for Single Phase Grid Connected Inverters

In this section, the conventional harmonic compensation methods for single phase GCIs in RRF are discussed. Firstly, the conventional harmonic

compensation methods are discussed in detail to exhibit the difficulties and complexity in the implementation. Then the proposed control method for the harmonic compensation is introduced and its implementation is detailed.

#### 3.1 Conventional Harmonic Compensation Method Based on RRF

Since the PI controller in RRF have a limited capability in compensating the low order ac ripple components, it is difficult to meet the harmonic standards such as IEEE 519 and P1547. Thus, the additional harmonic compensators are often added to the current control loop to eliminate the harmonics. There are two well-known harmonic elimination methods based on RRF.

One method is shown in Fig. 6. The PR controllers are employed in parallel with the current PI controller

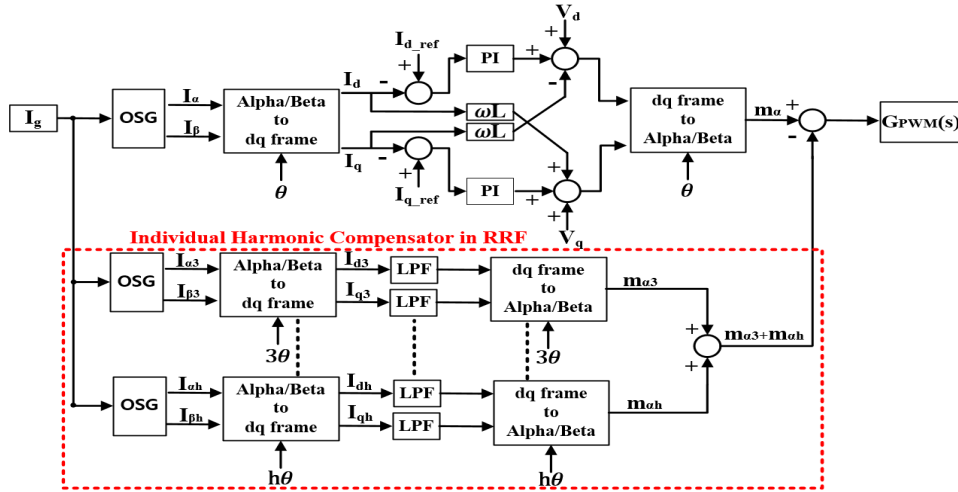


Fig. 8. Block diagram of the selective harmonic compensation method in RRF.

at the multiple of fundamental frequency. Each PR controller extracts the harmonic information from the current error and adds it to the output of the current regulator. Then the harmonic is compensated by the closed loop with negative feedback. The open loop transfer function of the current regulator with PR harmonic compensator can be expressed by Eq. (8).

$$G_i(s) = K_p + \frac{K_i}{s} + \sum_{h=2,4,6,\dots} \frac{K_{r,h}s}{s^2 + (h\omega_f)^2} \quad (8)$$

Where the  $K_p$  and  $K_i$  is the proportional and integral gain of the PI controller, respectively, and  $K_{r,h}$  is the resonant gain of the harmonic compensator.

However, as mentioned earlier, this control method has a problem that one harmonic in SRF appears as two different harmonics in the RRF. When the inverter current injected into the grid is composed of the fundamental and third harmonic component, it can be expressed in orthogonal form as shown in Eq. (9).

$$\begin{bmatrix} i_\alpha \\ i_\beta \end{bmatrix} = \begin{bmatrix} I_g(\cos\theta_g + \cos 3\theta_g) \\ I_g(\sin\theta_g + \sin 3\theta_g) \end{bmatrix} \quad (9)$$

Then the park transformation is applied to transform the orthogonal components of the grid current in the SRF into those in the RRF as shown in Eq. (10).

$$\begin{bmatrix} i_d \\ i_q \end{bmatrix} = \begin{bmatrix} \cos\theta_g & \sin\theta_g \\ -\sin\theta_g & \cos\theta_g \end{bmatrix} \begin{bmatrix} i_\alpha \\ i_\beta \end{bmatrix} \quad (10)$$

It can be found from Eq. (11) that an odd harmonic in the SRF appears as two different even harmonics in the RRF.

$$\begin{bmatrix} i_d \\ i_q \end{bmatrix} = \begin{bmatrix} I_g(1 + (\cos 2\theta_g) + (\cos 4\theta_g)) \\ I_g((\sin 2\theta_g) + (\sin 4\theta_g)) \end{bmatrix} \quad (11)$$

To verify the Eq. (11) the FFT analyses of the 3<sup>rd</sup> harmonic in SRF and RRF are shown in Fig. 7. It can be seen from the Fig. 7 that the 3<sup>rd</sup> harmonic in SRF appears as 2<sup>nd</sup> and 4<sup>th</sup> harmonics in RRF. Therefore, in order to compensate the 3<sup>rd</sup> harmonic in SRF, two different harmonic controllers are required at 2<sup>nd</sup> and 4<sup>th</sup> of the fundamental frequency. Therefore, it is difficult to compensate for the harmonics in the RRF since two compensators for a harmonic should be implemented. In addition, this technique requires a harmonic controller for each d and q axis, respectively, and it would further increase the complexity in the design of current controllers and hence the computational burden. As the SOGI composed of two low pass filters is used to generate the orthogonal signals from the grid current feedback, it accompanies an attenuation of the harmonic component. Therefore, it makes it difficult for the PR harmonic controllers to extract the accurate harmonic information from the grid feedback current.

The other difficulty in implementing the PR controller is to discretize the controller because it has a narrow band and infinite gain at the resonant frequency. Actually, a slight disagreement of the resonant poles cause a significant loss in terms of performance. When there is a small frequency deviation in the resonant frequency, the controller behaves like a proportional controller and it is not able to achieve zero steady-state error. The sensitivity of PR controller can be reduced to increase

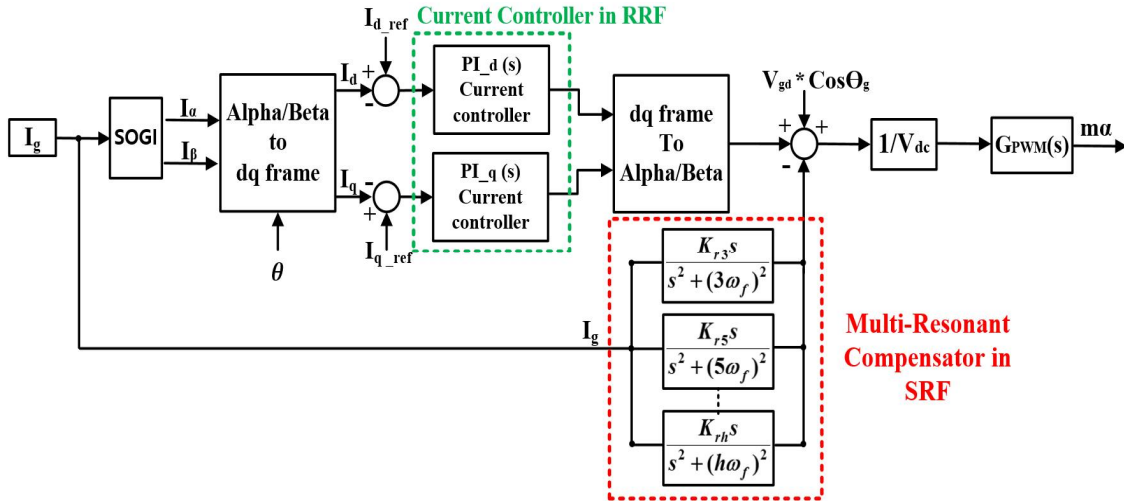


Fig. 9. Block diagram of the proposed harmonic compensation method.

the robustness to frequency variation by adding a damping factor. However, the damping factor should be selected carefully because inappropriate selection of the damping factor results in an amplification of the undesired frequencies and noise, which provides the detrimental effects to the control performance. Therefore, it is difficult to design and tune the PR controller to achieve the desirable performance.

In order to overcome this issue another method is proposed using multiple RRF for harmonic compensation as shown in Fig. 8. In this method multiple numbers of RRFs for each harmonic are used to regulate it by converting it to a dc component and the harmonic is compensated in a feedforward manner. The output current is measured and fed back to each RRF with different frequency. Each harmonic component appears as a dc term in its own frequency frame. It is advantageous that the harmonics can be regulated by a simple PI controller.

However, the main disadvantage of the method is that the dynamic characteristics of the harmonic compensation is not good enough due to the delay produced by the low pass filter. Moreover, the use of multiple number of RRFs and the associated computation blocks such as the low pass filters and frame transformation blocks result in the quite high complexity and hence the computational burden.

### 3.2 Proposed Harmonic Compensation Method Based on RRF

In this section a novel harmonic compensation method for a single phase GCI is proposed as shown

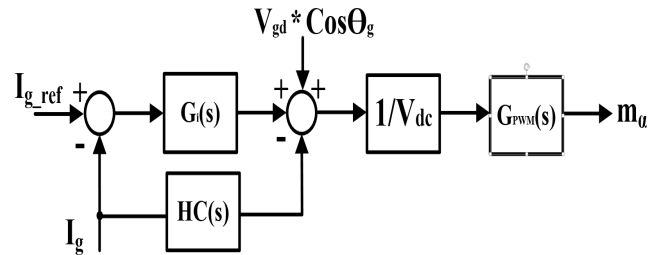


Fig. 10. Simplified block diagram of the proposed harmonic compensation method.

in Fig. 9. It can be regarded as a hybrid method which uses the RRF for the grid current control and the SRF for the harmonic compensation.

The simplified block diagram of the proposed technique is shown as Fig. 10, where the  $G_i(s)$  is the current tracking regulator and  $HC(s)$  is the harmonic compensator. In the proposed scheme, the grid current is regulated by the PI controller in the RRF and the PR controller deals with the current harmonics in the SRF.

The PR controller detects the harmonic information from the inverter current injected into the grid and it is added to the PWM voltage command after the park's transformation to compensate for the certain harmonic. The advantages of the propose method over the conventional methods include the simplicity in implementing the controller. Since the harmonic compensation is implemented in SRF there is no need for the transformation for the harmonic compensation. In addition only one controller needs to be implemented to compensate for a certain harmonic hence the computational burden can be further reduced as compared to the conventional methods.

Based on the system shown in Fig. 2 the dynamic equation of SPGCI can be described as

$$-m_a(s)V_{dc} + s(L_i + L_g)I_g + (R_i + R_g)I_g + V_g(s) = 0 \quad (12)$$

By rearranging Eq. (12) the grid current can be derived as:

$$I_g(s) = \frac{m_a(s)V_{dc} - V_g(s)}{(L_i + L_g)s + (R_i + R_g)} \quad (13)$$

The grid current can be written as:

$$I_g(s) = G_1(s)m_a(s) - G_2(s)V_g(s) \quad (14)$$

Where:

$$G_1(s) = \frac{V_{dc}}{(L_i + L_g)s + (R_i + R_g)}$$

$$G_2(s) = \frac{1}{(L_i + L_g)s + (R_i + R_g)}$$

From Fig. 10, the duty cycle dynamic equation for the proposed control technique can be written as follows.

$$m_a(s) = \{i_{g\_ref}G_i(s) - [G_i(s) + HC(s)]i_g\}G_{PWM}(s)/V_{dc}(s) \quad (15)$$

By substituting Eq. (15) into Eq. (14) the grid current dynamic equation can be expressed as,

$$I_g(s) = G_3(s)I_{g\_ref}(s) - G_4(s)V_g(s) \quad (16)$$

Where:

$$G_3(s) = \frac{G_1(s)G_i(s)G_{PWM}(s)/V_{dc}}{1 + T(s)}$$

$$G_4(s) = \frac{G_2(s)}{1 + T(s)}$$

The open loop gain  $T(s)$  can be derived from the Eq. (16) with the assumption that the decoupling terms are completely cancelled by the feedforward control and it has negligible effect on the performance of control system. It can be expressed as:

$$T(s) = G_1(s)(G_i(s) + HC(s))G_{PWM}/V_{dc} \quad (17)$$

The design of the current regulator  $G_i(s)$  determines the bandwidth and stability margin of the whole system. Ideally, the bandwidth of the closed

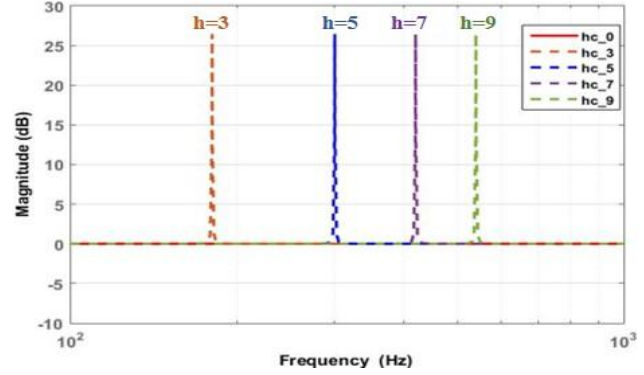


Fig. 11. Bode plot of the harmonic compensator at different h values.

loop system must be maximized by selecting a higher proportional gain  $k_p$  to obtain fast dynamic response and high disturbance rejection capability. A high gain, however, degrades the control system stability and decrease the noise immunity of the system. Consequently, the choice of the proportional gain  $k_p$  is a trade-off between the stability margin and the bandwidth of the system.

The bode plots of harmonic compensator with different h values are drawn in Fig. 11. As shown in the Fig. 11 the bode plot of the PR controller shows a high gain at the certain frequency. As a consequence, a certain harmonic of the inverter current can be extracted and used to compensate it by the negative feedback control loop. The design of the current controller is performed by using SISOTOOL in MATLAB software. At first the PI current regulator is designed in such a way to pass the harmonic component without attenuating it.

After design the PI current regulator, the PR controller is added with current regulator for the compensation of a specific frequency harmonic. In the design of PR harmonic controller  $K_r$  is the resonant gain of each controller. The higher value of  $K_r$  provides a higher selectivity of the harmonic component and hence it results in a better performance to compensate an individual current harmonic. However, it also reduces the system phase margin, resulting in an instability of the overall control system.

Therefore, there is a trade-off in selecting a value for  $K_r$  gain and the optimal  $K_r$  value needs to be found by the trial and error method.

In this paper the only the 3<sup>rd</sup> harmonic is compensated since it is the most dominant among other harmonic present in the output current. Based on



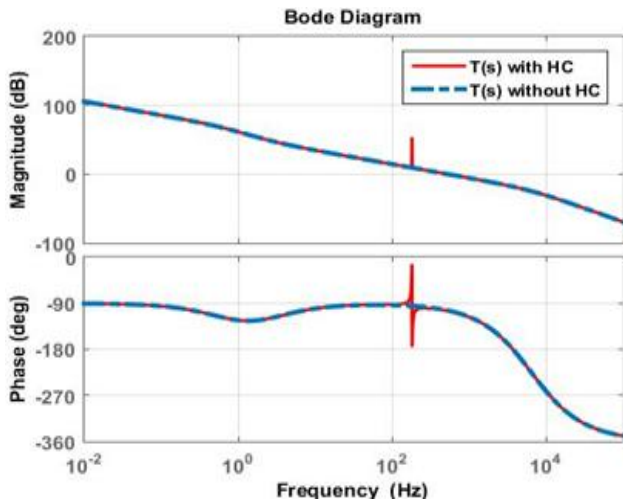


Fig. 12. Bode plot of the open loop gain  $T(s)$  with and without harmonic compensator.

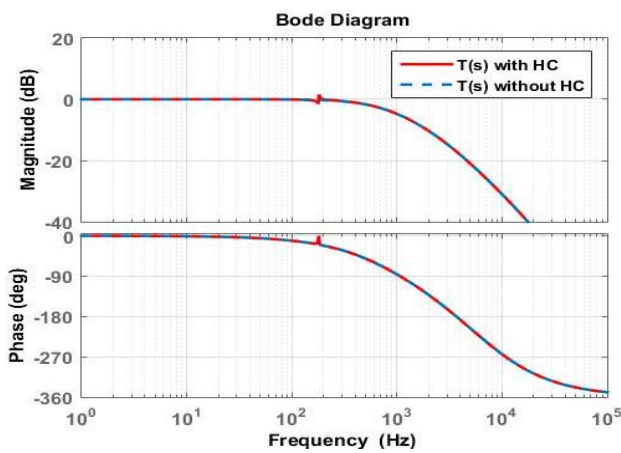


Fig. 13. Bode plot of the closed loop gain with and without harmonic compensator.

Eq. (17) the open loop and closed loop bode plot of the proposed system with and without harmonic compensator are shown in Fig. 12 and Fig. 13, respectively. In Fig. 12 and 13 the responses of the controller with and without HC are same but the only difference is the high gain at the 3<sup>rd</sup> harmonic frequency due to the PR controller.

#### 4. Simulation Results

In order to show the superior performance of the proposed method with respect to the conventional current control methods PSIM simulations are conducted. All the current control algorithms have been implemented for the performance comparison and the results are compared under the grid conditions with 2nd, 3rd and 5th harmonics of which magnitudes are 0.1%, 0.4% and 0.1% of the grid voltage,

TABLE I  
SYSTEM PARAMETER FOR SINGLE PHASE GRID CONNECTED INVETER

Parameters	Values
Rated Power ( $P_o$ )	5kW
Switching / Sampling frequency ( $f_{sw}$ )	10kHz
Dead time ( $t_d$ )	0.5 $\mu$ s
Inverter side inductor ( $L_i$ )	1.5mH
Grid side inductor ( $L_g$ )	1.5mH
Filter capacitor ( $C_f$ )	6.0 $\mu$ F
Damping resistor ( $R_d$ )	3.0 ohm
Inductor resistances ( $R_i+R_g$ )	0.15 $\Omega$
Grid voltage ( $V_g$ )	220Vrms
Grid frequency ( $f_g$ )	60Hz
DC link Voltage ( $V_{dc}$ )	400V
DC link Capacitor ( $C_{dc}$ )	3.0mF

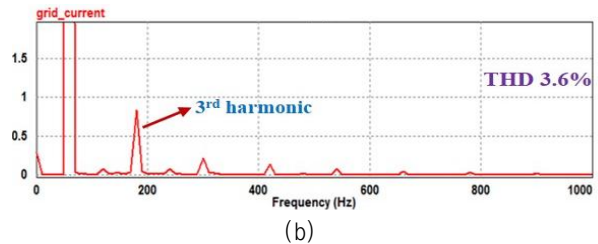
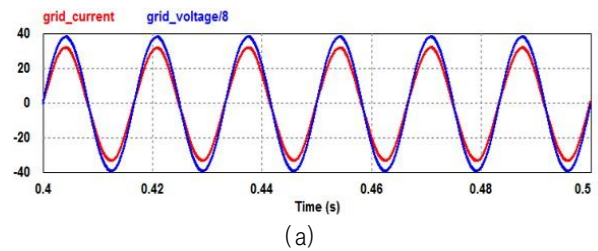


Fig. 14. Simulation results of a conventional harmonic compensation method at 5kW.

respectively. Here, the THD of the grid voltage is about 0.5% and the dead time is 0.5 $\mu$ s. The specification of the system is shown in Table I.

As already shown in Fig. 5 that the amplitude of 3rd harmonic is 1.96 A and the THD of the SPGCI with no harmonic control is 6.3%, which cannot meet IEEE Std. 519 and P1547.

Fig. 14 shows the performance of the inverter with the conventional harmonic compensation technique. As shown in Fig. 14, the amplitude of the 3rd harmonic component is reduced from 1.96 to 0.83A(58% reduction in the amplitude) and the output current THD is 3.6%, which can satisfy the harmonic standards.

Fig. 15 shows the performance of the inverter with the proposed technique. As shown in Fig. 15, the amplitude of the 3rd harmonic component is reduced from 1.96 to 0.09A(95% reduction in the amplitude)

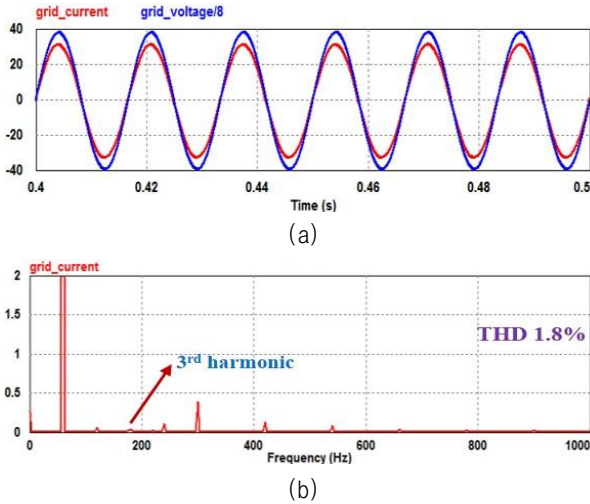


Fig. 15. Simulation results of the proposed harmonic compensation method at 5kW.

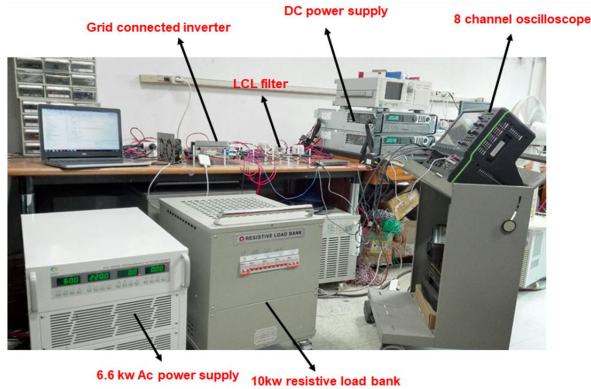


Fig. 16. Experimental setup of the SPGCI.

and the output current THD is 1.8%, which can satisfy the harmonic standards. The THD of the inverter is improved from 6.3% to 1.8% and 3rd harmonic component is reduced from 1.96A to 0.09A which is 95% reduction.

### 5. Experimental Results

To verify the superior performance of the proposed method a prototype of 5kW SPGCI has been built in the laboratory as shown in Fig. 16. The system parameters are given in Table I. The switching frequency is 10 kHz(fsw) and the unipolar PWM is used. The SPGCI is controlled by using a TI floating-point DSP TMS320F28335. All the current controllers are implemented by discretizing it with bi-linear transformation.

Fig. 17 shows the experimental results of the RRF current controller without harmonic compensator. It can be observed from Fig. 17 that the most dominant

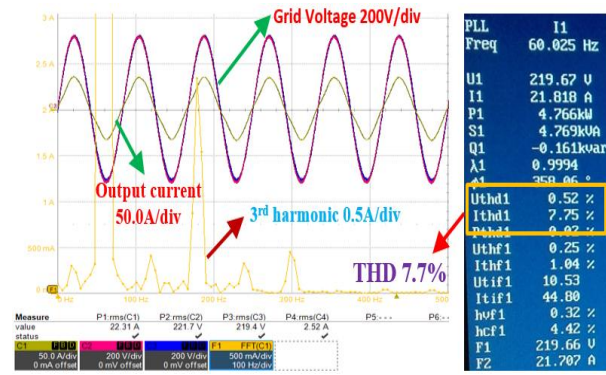


Fig. 17. Experimental results without a harmonic controller at 5kW.

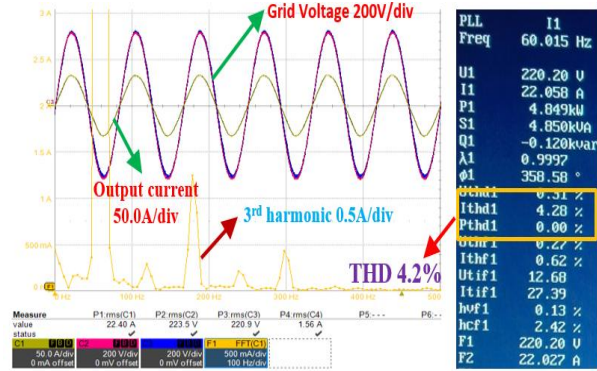


Fig. 18. Experimental results with a conventional harmonic controller at 5kW.

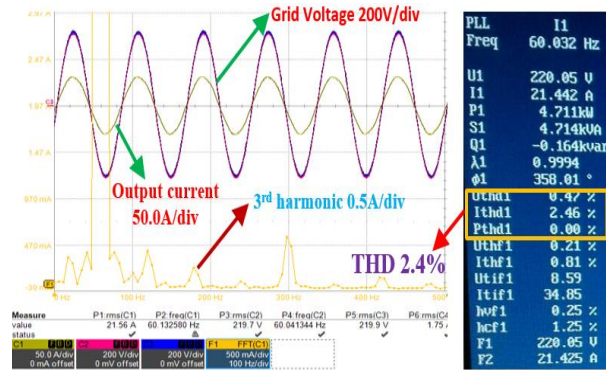


Fig. 19. Experimental results with the proposed harmonic controller at 5kW.

harmonic is 3rd harmonic of which magnitude is 2.4A and the output current THD is 7.75% which cannot satisfy the IEEE Std.519 and P1547.

Fig. 18 shows the experimental results of the RRF current controller with the conventional harmonic compensator. In the conventional harmonic compensation method, the 3rd harmonic in SRF is compensated by adding two harmonic controllers at 2nd and 4th harmonics. It can be observed from Fig. 18 that the

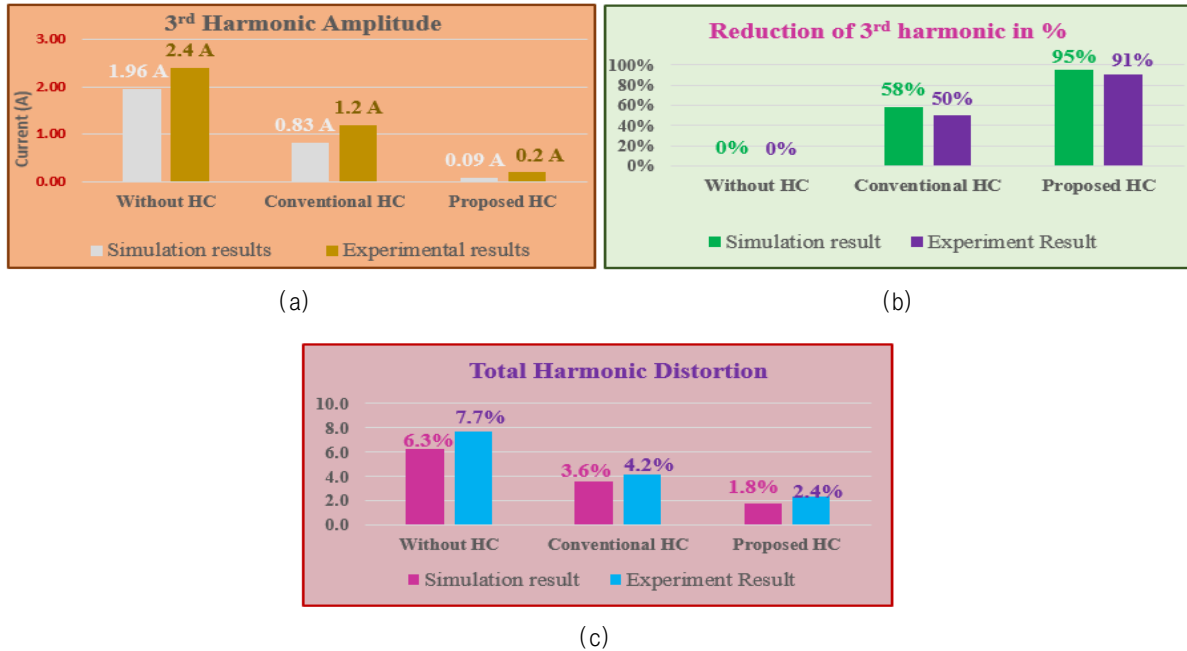


Fig. 20. Comparison of the conventional and the proposed harmonic compensator. (a) 3rd harmonic reduction, (b) harmonic reduction rate, (c) Total Harmonic Distortion.

THD is reduced from 7.75% to 4.2% and 3rd harmonic is reduced from 2.4A to 1.2A(50% reduction in magnitude) as compared to the results with no harmonic controller.

Fig. 19 shows the experimental results of the RRF current controller with the proposed harmonic compensator. It can be observed from Fig. 19 that the THD is reduced from 7.75% to 2.4% and 3rd harmonic is reduced from 2.4A to 0.2A(91% reduction in magnitude) as compared to the results with no harmonic controller.

Therefore, it can be confirmed with the experimental results that the harmonic attenuation performance of the proposed method is better than that of the conventional methods. The simulation and experiment results with conventional and proposed harmonic compensation methods are drawn by using bar chart in Fig. 20.

## 6. Conclusion

In this paper, a new harmonic compensation method to eliminate the low order harmonics is proposed and its validity has been proved by the simulation and experiments. The proposed current controller has been developed with the current regulator on RRF while the harmonic compensator is implemented with a PR controller in SRF. It has been verified through the

experiments that the proposed harmonic compensation technique is able to effectively eliminate the low order harmonics and superior to the conventional one in terms of harmonic rejections. Hence the THD of the SPGCI can be significantly improved to meet the THD of it under the distorted grid condition. Another advantage of the proposed method is that it can be implemented in a low cost CPU since the its computational burden is lower than that of the conventional method.

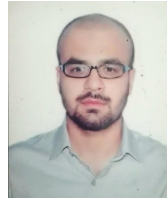
This research was supported by Korea Electric Power Corporation. (Grant number : R17XA05-42)

## References

- [1] W. Sinsukthavorn, E. Ortjohann, A. Mohd, N. Hamsic, and D. Morton, "Control strategy for three-/four wire inverter based distributed generation," *IEEE Trans. Ind. Electron.*, Vol. 59, No. 10, pp. 3890-3899, Oct. 2012.
- [2] C. Trujillo, D. Velasco, G. Garcera, E. Figueres, and J. Guacaneme, "Reconfigurable control scheme for a PV micro inverter working in both grid-connected and island modes," *IEEE Trans. Ind. Electron.*, Vol. 60, No. 4, pp. 1582-1595, Apr. 2013.
- [3] C. G. C. Branco, R. P. Torrico-Bascope, C. M. T. Cruz, and F. K. de A Lima, "Proposal of three-phase high-frequency transformer isolation UPS topologies for

- distributed generation applications,” *IEEE Trans. Ind. Electron.*, Vol. 60, No. 4, pp. 1520–1531, Apr. 2013.
- [4] R. J. Wai, C. Y. Lin, Y. C. Huang, and Y. R. Chang, “Design of high-performance stand-alone and grid-connected inverter for distributed generation applications,” *IEEE Trans. Ind. Electron.*, Vol. 60, No. 4, pp. 1542–1555, Apr. 2013.
- [5] S. B. Kjaer, J. K. Pedersen, and F. Blaabjerg, “A review of single-phase grid-connected inverters for photovoltaic modules,” *IEEE Trans. Ind. Appl.*, Vol. 41, No. 5, pp. 1292–1306, Sep./Oct. 2005.
- [6] G. He, D. Xu, and M. Chen, “A novel control strategy of suppressing DC current injection to the grid for single-phase PV inverter,” *IEEE Trans. Power Electron.*, Vol. 30, No. 3, pp. 1266–1274, Mar. 2015.
- [7] IEEE15471, “IEEE standard for interconnecting distributed resources with electric power systems,” 2005.
- [8] IEEE Standard 519-1992, “IEEE Recommended Practices and Requirements for Harmonic Control in Electrical Power Systems,” 1992.
- [9] Y. A. R. I. Mohamed and E. F. El-Saadany, “A control scheme for PWM voltage-source distributed-generation inverters for fast load voltage regulation and effective mitigation of unbalanced voltage disturbances,” *IEEE Transactions on Industrial Electronics*, Vol. 55, No. 5, pp. 2072–2084, May 2008.
- [10] X. Zhang, Y. Wang, C. Yu, L. Guo, and R. Cao, “Hysteresis model predictive control for high-power grid-connected inverters with output LCL filter,” *IEEE Transactions on Industrial Electronics*, Vol. 63, No. 1, pp. 246–256, Jan. 2016.
- [11] A. Timbus, M. Liserre, R. Teodorescu, P. Rodriguez, and F. Blaabjerg, “Evaluation of current controllers for distributed power generation systems,” *IEEE Trans. Power Electron.*, Vol. 24, No. 3, pp. 654–664, Mar. 2009.
- [12] M. Castilla, J. Miret, A. Camacho, J. Matas, and L.G. de Vicuna, “Reduction of current harmonic distortion in three-phase grid connected photovoltaic inverters via resonant current control,” *IEEE Trans. Ind. Electron.*, Vol. 60, No. 4, pp. 1464–1472, Apr. 2013.
- [13] Q. N. Trinh and H. H. Lee, “An enhanced grid current compensator for grid-connected distributed generation under nonlinear loads and grid voltage distortions,” *IEEE Transactions on Industrial Electronics*, Vol. 61, No. 12, pp. 6528–6537, Dec. 2014.
- [14] R. Teodorescu, F. Blaabjerg, M. Liserre, and P. C. Loh, “Proportional resonant controllers and filters for grid-connected voltage-source converters,” *Proc. Inst. Elect. Eng. – Electr. Power Appl.*, Vol. 153, No. 5, pp. 750–762, Sep. 2006.
- [15] G. Shen, X. Zhu, J. Zhang, and D. Xu, “A new feedback method for PR current control of LCL-filter based grid-connected inverter,” *IEEE Trans. Ind. Electron.*, Vol. 57, No. 6, pp. 2033–2041, Jun. 2010.
- [16] J. Dannehl, C. Wessels, and F. W. Fuchs, “Limitations of voltage-oriented PI current control of grid-connected PWM rectifiers with LCL filters,” *IEEE Trans. Ind. Electron.*, Vol. 56, No. 2, pp. 380–388, Feb. 2009.
- [17] D. N. Zmood, D. G. Holmes, and G. H. Bode, “Frequency-domain analysis of three-phase linear current regulators,” *IEEE Trans. Ind. Appl.*, Vol. 37, No. 2, pp. 601–610, Mar./Apr. 2001.
- [18] D. N. Zmood and D. G. Holmes, “Stationary frame current regulation of PWM inverters with zero steady-state error,” *IEEE Trans. Power Electron.*, Vol. 18, No. 3, pp. 814–822, May 2000.
- [19] T. L. Lee and S. H. Hu, “Resonant current compensator with enhancement of harmonic impedance for LCL-filter based active rectifiers,” in *Proc. IEEE APEC*, pp. 1538–1543, 2011.
- [20] R. Teodorescu et al., “Proportional-resonant controllers and filters for grid connected voltage-source converters,” *IEE Proc. – Elect. Power Appl.*, Vol. 153, No. 5, pp. 750–762, Sep. 2006.
- [21] H. Nazifi and A. Radan, “Current control assisted and non-ideal proportional-resonant voltage controller for four-leg three-phase inverters with time-variant loads,” in *Proc. 4th Power Electron. Drive Syst. Technol. Conf.*, pp. 355–360, 2013.
- [22] M. Liserre, F. Blaabjerg, and S. Hansen, “Design and control of an LCL-filter-based three-phase active rectifier,” *IEEE Trans. Ind. Appl.*, Vol. 41, No. 5, pp. 1281–1291, Sep./Oct. 2005.
- [23] E. Twining and D. G. Holmes, “Grid current regulation of a three-phase voltage source inverter with an LCL input filter,” *IEEE Trans. Power. Electron.*, Vol. 18, No. 3, pp. 888–895, May. 2003.
- [24] M. P. Kazmierkowski and L. Malesani, “Current control techniques for three-phase voltage-source PWM converters: a survey,” *IEEE Trans. Ind. Electron.*, Vol. 45, No. 5, pp. 691–703, Oct. 1998.
- [25] M. Saitou and T. Shimizu, “Generalized theory of instantaneous active and reactive powers in single-phase circuits based on Hilbert transform,” in *Proc. 33rd Annu. IEEE PESC*, pp. 1419–1424, Jun. 2002.
- [26] I. Carugati, P. Donato, S. Maestri, D. Carrica, and M. Benedetti, “Frequency adaptive PLL for polluted single-phase grids,” *IEEE Trans. Power Electron.*, Vol. 27, No. 5, pp. 2396–2404, May 2012.
- [27] S. M. Silva, B. M. Lopes, B. J. C. Filho, R. P. Campana, and W. C. Boaventura, “Performance evaluation of PLL algorithms for single phase grid-connected systems,” in *39th Conf. Rec. IEEE IAS Annu. Meeting*, Vol. 4, pp. 2259–2263, Oct. 2004.
- [28] R. Zhang, M. Cardinal, P. Szczesny, and M. Dame, “A grid simulator with control of single-phase power converters in D-Q rotating frame,” in *Proc. IEEE Power Electron. Spec. Conf.*, pp. 1431–1436, 2002.

- [29] R. Y. Kim, S. Y. Choi, and I. Y. Suh, "Instantaneous control of average power for grid tie inverter using single phase D-Q rotating frame with all pass filter," in *Proc. IEEE Ind. Electron. Conf.*, Busan, Korea, pp. 274-279, Nov. 2004.
- [30] M. Ciobotaru, R. Teodorescu, and F. Blaabjerg, "A new single-phase PLL structure based on second order generalized integrator," in *Proc. 37th IEEE Power Electronics Specialists Conference*, pp 1-6, 2006.
- [31] M. Liserre, R. Teodorescu, and F. Blaabjerg, "Multiple harmonic control for three phase grid converter system with the use of PI-RES current controller in rotating frame," *IEEE Trans. Power Electron.*, Vol. 21, No. 3, May 2006.
- [32] E. S. Kim, U. S. Seong, J. S. Lee, and S. H. Hwang, "Compensation of dead time effects in grid-tie single phase inverter using SOGI," in *Applied Power Electronic Conference and Exposition (APEC)*, pp. 2633-2637, 2017.
- [33] D. C. Gaona, R. P. Alzola, J. L. M. Morales, M. Ordonez, O. A. Lara, and W. E. Leithead, "Fast selective harmonic mitigation in multifunctionla inverters using internal model controllers and synchronous reference frame," *IEEE Trans. Ind. Electron.*, Vol. 64, No. 8, Aug. 2017.



### **Reyyan Ahmad Khan**

He was born on April 28, 1993 in Islamabad, Pakistan. He received his B.S. in electronic engineering from International Islamic University Islamabad, Pakistan in 2011. He received his M.S. in electrical engineering at Soongsil University, Republic of Korea in 2018. He is currently working in Advanced Drive Technology as an Assistant Engineer/R&D center.



### **Woojin Choi**

He was born in Seoul, Korea, in 1967. He received the B.S. and M.S. degrees from Soongsil University, Seoul, Korea, in 1990 and 1995, respectively, and the Ph.D. degree from Texas A&M University, College Station, TX, in 2004, all in electrical engineering. From 1995 to 1998, he was a Research Engineer at the central R&D division of Daewoo Heavy Industries. In 2005, he joined the School of Electrical Engineering, Soongsil University, Seoul, South Korea.